

Patient-specific simulation of the blood flow in an aortic dissection for clinical support including an efficient method to represent the motion of the intimal flap and vessel wall: A case study

Mirko Bonfanti^{1,*}, Mona Alimohammadi¹, Shervanthi Homer-Vanniasinkam^{1,2},
Vanessa Díaz-Zuccarini^{1,*}.

1 Department of Mechanical Engineering, University College London, UK

2 Division of Surgery and Interventional Science, University College London, UK

* Correspondence: mirko.bonfanti.15@ucl.ac.uk, v.diaz@ucl.ac.uk, Mechanical Engineering, University College London, Torrington Place, London WC1E 7JE, UK.

1. Introduction

Aortic Dissection (AD) is a life-threatening vascular condition characterised by the separation of the layers of the aortic wall. A tear in the intima layer allows the blood to flow within the aortic wall inducing the formation of the dissection, which finally results in two distinct flow channels, the true lumen (TL) and the false lumen (FL), separated by the so called intimal flap (IF) [1].

The medical management of Stanford type B dissections (i.e. ADs involving only the descending aorta) must undergo a clinical decision-making process [2]. In case of complications the surgical intervention is the preferred choice, whereas uncomplicated ADs are usually managed conservatively by controlling the blood pressure [3]. However, the long-term prognosis of medically treated ADs remains poor, with delayed aortic dilation and late-term complications reported in 25-50% of the cases within 5 years [4].

Clinical decisions regarding diagnosis, management and treatment of AD are incredibly patient-specific and difficult; aortic dissection is not diagnosed on its initial presentation in 15-43% of cases [5,6]; in fact, one expert claims that "difficulty in diagnosis, delayed diagnosis or failure to diagnose are so common as to approach the norm for this disease, even in the best hands..." [7]. Initial management of diagnosed or highly suspected acute aortic dissection focuses on pain control, heart rate and then blood pressure management, and immediate surgical consultation (typically by considering whether or not stenting the upper tear). It is an ever-increasing problem; when the condition is identified, therapy is driven by a set of key principles and *plagued by several management pitfalls*. [8]

Patient-specific computational fluid dynamics (CFD) may be able to help the decision-making process around the disease and to aid the identification of patients prone to adverse outcomes by providing detailed information about haemodynamic factors (typically pressure and flow). Moreover, numerical models may support clinicians by virtually simulating different interventional strategies [9].

A common approach adopted in CFD is the assumption of a 3D rigid model, which neglects the effect exerted on the fluid dynamics by the vessel wall compliance and IF motion. This assumption may have a major impact on CFD results, in particular in acute ADs which can involve significant IF motion [10]. Currently in the literature only a few studies on AD account for wall motion by employing fluid-structure interaction (FSI) techniques [11,12]. FSI couples CFD simulations with finite element modelling (FE) of the aortic wall; however, this method is subject to additional modelling hypotheses regarding the mechanical properties of the vessel, which are unknown for the pathologic dissected aorta and may vary for each patient, usually demanding a high computational cost to be resolved.

In order to tackle this problem, this study presents a flexible and computationally efficient method to account for the motion of the intimal flap and vessel wall in AD CFD simulations, by making use of non-invasive and patient-specific measurements (e.g. via 2D PC-MRI or 4D Flow MRI). A case study was analysed using displacement and haemodynamic data generated from a patient-specific simulation (FSI) of a type B AD, which initially involved invasive pressure measurements and is presented elsewhere [12].

2. Materials and Methods

2.1. Description of the method

The proposed moving-mesh (MM) method allows the motion of the 3D-model boundaries in a CFD framework by means of deformable mesh, avoiding the computation of detailed mechanical analysis in the

biological tissue. As a first approximation, it is assumed that the displacements of the aortic external wall and IF follow the local surface-normal direction, and are linearly related to the fluid forces. The displacement δ_i [m] of each mesh node i on the external vessel wall is prescribed by Eq. 1:

$$\delta_i = \frac{p_i - \bar{p}}{K_i} \vec{n}_i \quad (1)$$

where p_i [Pa] is the pressure at node i ; \bar{p} [Pa] is the external pressure set as equal to the diastolic pressure; K_i [N/m³] is the elastic coefficient set at node i ; \vec{n}_i is the local unit normal vector in the outward direction. The IF, modelled as a zero-thickness membrane, is discretized into a number of patches (i.e. surface regions); the displacement δ_j [m] of each mesh node on patch j is prescribed by Eq. 2:

$$\delta_j = \frac{\vec{F}_j^{\text{tm}}}{K_j A_j} \quad (2)$$

where \vec{F}_j^{tm} [N] is the surface normal-transmural force (TMF) on patch j , taking into account the viscous and pressure forces acting on both TL and FL sides of the IF patch; A_j [m²] is the surface area of patch j ; K_j [N/m³] is the elastic coefficient assigned to patch j . For each patch, K_j can assume two values, namely K_j^{FL} and K_j^{TL} depending on whether \vec{F}_j^{tm} points in the direction of the FL or the TL, respectively. Thus, it is possible to account for potential different mechanical behaviour of the IF in case of extension (i.e. TL expansion) or contraction (i.e. TL compression), as highlighted by Karmonik et al. [13]. The tuning of K_i and K_j is based on patient-specific displacement data.

2.2. Computational Fluid Dynamics

As previously stated, as a proof of concept and for validation purposes, the MM method was applied to a case study investigated in previous work by Alimohammadi et al. [12] with an FSI methodology. The study was ethically approved (NHS Health Research Authority, ref: 13/EM/0143). The MM model was set up exploiting the displacement data obtained from the FSI simulation [12] (details in section 2.3); the CFD results of the two models were then compared so as to verify the reliability of the proposed method.

Table 1: Boundary conditions used for the CFD simulation. Fig. 1a shows the position of the boundaries.

Boundary	Fluid Flow	Mesh Motion
AA – Ascending aorta	Flow inlet as in [12] – Fig. 1b	Parallel to boundary surface
BT – Brachiocephalic trunk	RCR Windkessel – Parameters as in [12, 14]	Parallel to boundary surface
LCC – Left common carotid artery	RCR Windkessel – Parameters as in [12, 14]	Parallel to boundary surface
LS – Left subclavian artery	RCR Windkessel – Parameters as in [12, 14]	Parallel to boundary surface
DA – Descending aorta	RCR Windkessel – Parameters as in [12, 14]	Parallel to boundary surface
External vessel wall	No slip	Specified displacement as per Eq. 1
IF – Intimal flap	No slip	Specified displacement as per Eq. 2

The 3D domain was built upon the segmented geometry used for the FSI model, representing an acute type-B AD of a 54-year-old female patient (details on the image acquisition can be found in [12]). The surface of the IF was discretised in about 200 patches with the aid of the +NURBS module of ScanIP image-processing software (Simpleware Ltd., Exeter, UK). The fluid volume was discretised with a tetrahedral mesh in the core region and 7 prism layers at both IF sides and vessel wall, using ICEM-CFD (ANSYS Inc., Canonberg, USA). The final mesh consisted of about 483,000 elements with an element size comparable to the mesh used in [12]. In order to perform a meaningful comparison, the same CFD boundary conditions (BCs) and fluid flow model employed in [12] were applied to the MM model. In particular, blood was modelled as an incompressible fluid with density of 1056 kg/m³ and non-Newtonian viscosity described by the Carreau-Yasuda model, with parameters from [15]. The shear-stress transport turbulence model was applied with 1% turbulence intensity at the inlet [12]. The fluid flow and mesh motion BCs are detailed in Table 1. The Navier-Stokes equations were solved with ANSYS-CFX 17.0 with a time step of 0.01 s. For each simulation, the periodic steady-state was achieved within 3 cardiac cycles after appropriate initialisation and the results of the last cycle were used for the analysis.

2.3. Model-tuning procedure based on displacement data

The tuning procedure described here employs data obtained from an FSI simulation [12] and a similar approach can be adopted using clinically-obtained motion data (e.g. 2D PC-MRI).

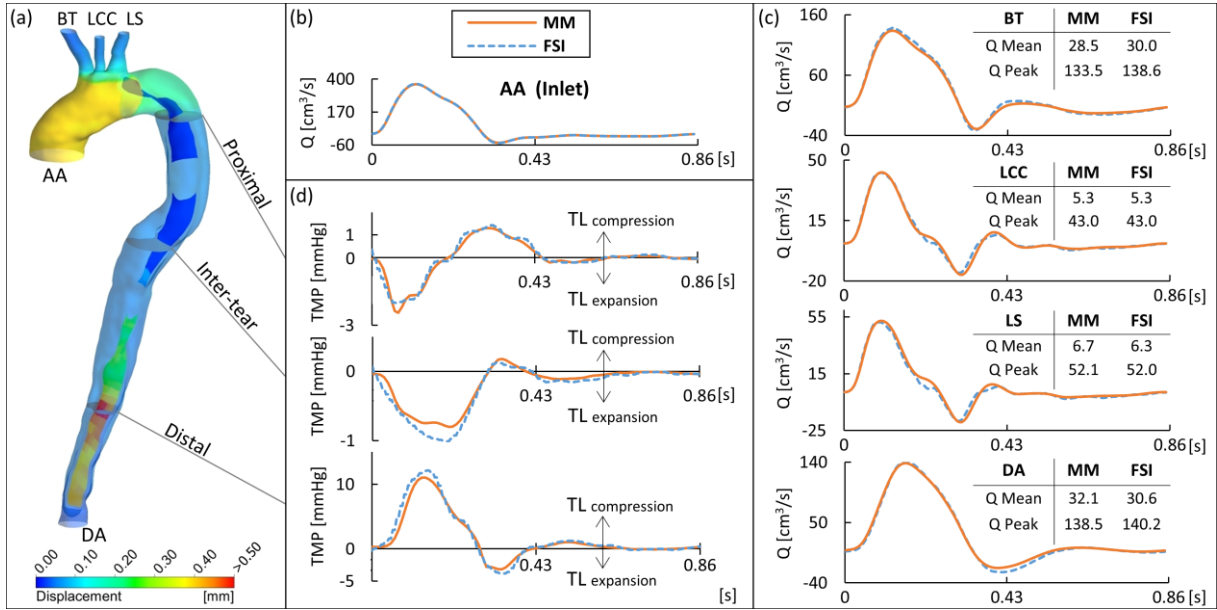


Figure 1: (a) Displacement of vessel wall and IF at peak-systole; (b) Flow rate set at model inlet; (c-d) Comparison between simulation data obtained with FSI and moving mesh (MM) method: flow rate curves at model outlets (c), and transmural pressure (TMP) across the IF at proximal, inter-tear, and distal regions.

Parameter K_i is tuned in order to simulate the compliance of the aorta in the CFD model. The external wall is divided in regions (in this case: ascending aorta, upper aortic branches, and descending dissected aorta), each with a wall distensibility \mathcal{D}_k [Pa⁻¹] estimated with Eq. 3 [16]:

$$\mathcal{D}_k = \frac{\Delta A_k}{A_k^0 \Delta p_k} \quad (3)$$

where ΔA_k [m] is the difference between the maximum and minimum area over the cardiac cycle of a vessel cross-section slice in region k , in this case measured from FSI results; A_k^0 [m] is the minimum cross-section area; Δp_k [Pa] is the difference between the maximum and minimum average cross-section pressure calculated with the CFD simulation. Parameter K_i is related to \mathcal{D}_k via Eq. 4, where A_i^0 [m] is the minimum cross-section area of the vessel at the location of node i :

$$\forall \text{ nodes } i \in \text{region } k: K_i = \frac{2}{\mathcal{D}_k} \sqrt{\frac{\pi}{A_i^0}} \quad (4)$$

Parameter K_j is tuned so as to model the IF mechanical response to the TMF. A number of sample patches, amongst those into which the IF is discretized, are selected (in this case 15 patches). The maximum IF displacement through FL ($\delta_j^{\text{FL,max}}$) and TL ($\delta_j^{\text{TL,max}}$) over a cardiac cycle are measured from FSI results at the location of each selected patch. Thus, K_j^{FL} and K_j^{TL} are calculated via Eq. 5:

$$K_j^{\text{FL}} = \frac{F_j^{\text{FL,max}}}{\delta_j^{\text{FL,max}} A_j} \quad ; \quad K_j^{\text{TL}} = \frac{F_j^{\text{TL,max}}}{\delta_j^{\text{TL,max}} A_j} \quad (5)$$

where $F_j^{\text{FL,max}}$ and $F_j^{\text{TL,max}}$ [N] are obtained with CFD, and represent the maximum magnitude of the TMF on patch j , when pointing to FL or TL, respectively. K_j values for the remaining patches are interpolated from those calculated for the sample patches with MATLAB (Mathworks, Natick, USA). The variables acquired from CFD (i.e. Δp_k , $F_j^{\text{FL,max}}$ and $F_j^{\text{TL,max}}$) employed for the tuning procedure are obtained from a rigid-wall simulation. In this study, an appropriate match between the obtained displacement and the target FSI data was achieved with no need to iterate the tuning procedure.

3. Results

The displacement results at peak-systole obtained with the MM model are shown in Fig. 1a. It can be seen there is an expansion of the ascending aorta due to the vessel compliance, and a displacement up to 0.6 mm in the distal part of the IF, where the transmural pressure (TMP) is higher compared to the proximal and inter-tear regions (Fig. 1d). Fluid dynamics results obtained with the MM and FSI simulations are in good agreement. As shown in Fig. 1d, the TMP curves along the IF are well-matched throughout the cardiac cycle,

with a maximum difference of 0.2 mmHg in the inter-tear region of the IF. TMP is an important and clinically relevant information which drives the movement of the IF [10], and consequent TL compression or expansion. Also the flow rate (Q) at each domain outlet is in good agreement during the cardiac cycle (Fig. 1c): there is no phase-lag between the Q waves obtained with the MM and the FSI, and the difference between the mean flow is only of -1.5, 0.02, 0.5, 1.5 cm³/s at BT, LCC, LS and DA, resulting in relative errors of -5.0, 0.3, 7.5 and 5.0%, respectively. It is worth noting that no flow or pressure curves are imposed at the domain boundaries, apart from the flow rate wave at the domain inlet (Fig. 1b).

Table 2: Computational cost: MM vs. FSI.

Method	Mesh: # elements (# nodes)	Simulation time*
MM	Fluid: 483,126 (217,512)	16.5 h/cycle
FSI	Fluid: 233,591 (90,178) Solid: 48,433 (92,958)	37 h/cycle

*Simulations run on a workstation Intel Xeon E5, 8 cores, 32 GB RAM.

4. Discussion and Conclusions

Through this case study, this paper proposes a valid, new and computationally efficient method (compared to FSI) to account for wall motion in CFD simulations of AD. The good match obtained between MM and FSI results suggests that the MM method is able to capture the relevant features of the vessel wall motion. The purpose of the method is not to study in detail the deformation and stress arisen in the vessel tissue, as done by FSI techniques, but to take account of the effects exerted on the fluid dynamics by the motion of the vessel wall. These effects usually consist in a relevant phase-lag of the blood flow and in a reduction of peak flow rates due to the arterial compliance, and cannot be caught by rigid wall simulations as shown by Dillon-Murphy et al. [17].

Compared to FSI, the MM method has the advantage to be less computationally expensive (Tab. 2) and easier to implement, which are critical features in the context of clinical use. Moreover it can be easily tuned with patient-specific vessel motion data obtained non-invasively in the clinic (e.g. via 2D PC-MRI), thus reducing possible errors introduced by using constitutive models with parameters taken from the literature. Since the mesh motion is not imposed, but rather *modelled via simple linear equations* relating the fluid forces to the displacement of the boundaries, once the parameters have been tuned, the model can be used to simulate different haemodynamic conditions, for instance, allowing the evaluation of possible treatment strategies.

5. Acknowledgements

This project has received funding from the European Union's Horizon 2020 research and innovation programme under the Marie Skłodowska-Curie grant agreement No 642612.

6. References

1. Hagan GH et al., JAMA 2000;283(7):897-903
2. Nienaber CA and Clough RE, Lancet 2015;385:800-811
3. Goldfinger JZ et al., J. Am. Coll. Cardiol. 2014;64:1725-39
4. Doyle BJ et al., Ann. Biomed. Eng. 2016;44(1):71-83
5. Hansen MS et al., Am. J. Cardiol. 2007;99(6):852-856.
6. Sullivan PR et al., Am. J. Emerg. Med. 2000;18(1):46-50.
7. Eleftheriades JA et al., Cardiology 2008;109(4):263-272.
8. Strayer RJ et al., Curr. Cardiol. Rev 2012;8:152-157
9. Taylor CA and Figueroa CA, Annu. Rev. Biomed. Eng. 2009;11:109-34
10. Yang S et al., PLoS ONE 2014;9(2):e87664
11. Qiao A et al., Comput. Methods Biomech. Biomed. Engin. 2015;18(11):1173-1180
12. Alimohammadi et al. Biomed. Eng. Online 2015;14:34
13. Karmonik C et al., J. Vasc. Surg. 2012;55:1419-26
14. Alimohammadi M et al., Med. Eng. Phys. 2014;36:275-284
15. Gijssen F et al., J. Biomech. 1999;32:601-8
16. Ganten et al., Eur. J. Radiol. 2009;72:146-153
17. Dillon-Murphy D et al., Biomech. Model. Mechanobiol. 2015;1-20